ORIGINAL RESEARCH

Identification of Immuno-Inflammation-Related Biomarkers for Acute Myocardial Infarction Based on Bioinformatics

Hongjun You (iD), Mengya Dong (iD)

Department of Cardiovascular Medicine, Shaanxi Provincial People's Hospital, Xi'an, Shaanxi, 710068, People's Republic of China

Correspondence: Mengya Dong, Department of Cardiovascular Medicine, Shaanxi Provincial People's Hospital, Xi'an, Shaanxi, 710068, People's Republic of China, Tel +86-15802943974, Email 405895903@qq.com

Purpose: Previous studies have confirmed that inflammation and immunity are involved in the pathogenesis of acute myocardial infarction (AMI). However, only few related genes are identified as biomarkers for the diagnosis and treatment of AMI.

Patients and Methods: GSE48060 and GSE60993 datasets were retrieved from Gene Expression Omnibus. The differentially expressed immuno-inflammation-related genes (DEIIRGs) were obtained from GSE48060, and the biomarkers for AMI were screened and validated using the "Neuralnet" package and GSE60993 dataset. Further, the biomarker-based nomogram was constructed, and miRNAs, transcription factors (TFs), and potential drugs targeting the biomarkers were explored. Furthermore, immune infiltration analysis was analyzed in AMI. Finally, the biomarkers were verified by assessing their mRNA levels using real-time quantitative PCR (RT-qPCR).

Results: First, eight biomarkers were screened via bioinformatics, and the artificial neural network model indicated a higher prediction accuracy for AMI even in the validation dataset. Nomogram had accurate forecasting ability for AMI as well. The TFs GTF2I, PHOX2B, RUNX1, and FOS targeting hsa-miR-1297 could regulate the expressions of *ADM* and *CBLB*, and *RORA* could effectively interact with melatonin and citalopram. RT-qPCR results for ADM, PI3, MMP9, NRG1 and CBLB were consistent with those of bioinformatic analysis.

Conclusion: In conclusion, eight key immuno-inflammation-related genes, namely, *SH2D1B, ADM, PI3, MMP9, NRG1, CBLB, RORA*, and *FASLG*, may serve as the potential biomarkers for AMI, in which the downregulation of *CBLB* and upregulation of *ADM, PI3*, and *NRG1* in AMI was detected for the first time, providing a new strategy for the diagnosis and treatment of AMI.

Keywords: acute myocardial infarction, immune-related gene, inflammation-related gene, biomarker, nomogram

Introduction

Acute myocardial infarction (AMI) is the sudden irreversible necrosis of heart muscle, which commonly results from atherosclerotic plaque disruption and subsequent interruption of blood flow.[1] It is one of the heart diseases with the highest prevalence and incidence and brings enormous health and financial burdens.[2] Despite the rapid development of pharmacological and invasive treatments for AMI, particularly percutaneous coronary interventions, the admission and mortality rates are still high.[3,4] The progression of AMI to left ventricular dilatation, heart failure (HF), and sudden cardiac death still cannot be controlled.[5] Therefore, it is necessary and important to explore the pathogenesis of AMI.

Inflammation and metabolic disturbance are well-accepted underlying mechanisms of AMI, and significant evidence supports that inflammation and immunity have central roles in the development and progression of AMI.[6,7] The initial acute inflammatory response in AMI is triggered by innate immune response induced by damaged myocardial cells. The active innate immune system causes the infiltration of immune cells into ischemic heart tissue and coordinates the original proinflammatory responses.[8] Based on these aspects, a variety of machine learning algorithms have been integrated to identify novel diagnostic biomarkers in AMI to characterize the possible association between biomarkers and immune cell infiltration status. For example, Li et al integrated weighted gene co-expression network analysis

(WGCNA) and single-sample gene set enrichment analysis (ssGSEA) to identify candidate genes in AMI progression.[9] Immune-related genes were conducted to screen diagnostic biomarkers relevant to the pathological process of the AMI.[10] On the other hand, Wang et al identified eight miRNAs with high clinical applicability to distinguish patients with AMI from non-AMI individuals.[11] Meanwhile, there were few studies on the combination of inflammatory-related genes and immune-related genes to explore the biomarkers related to AMI recognition.

In the study, the key immuno-inflammation-related genes in AMI were identified via multiple bioinformatic methods from public databases. Enrichment analysis, immune infiltration analysis, and TF–miRNA–mRNA regulatory network analysis were conducted to assess the molecular mechanism of immuno-inflammation-related genes playing roles in AMI. In addition, drugs targeting key genes were evaluated for their ability to act as drug targets using a drug database. Our study provided novel potential biomarkers of AMI and strategies for the diagnosis and treatment of AMI.

Materials and Methods
Data Collection
We downloaded the transcriptome data of GSE48060 and GSE60993 from the GEO (https://www.ncbi.nlm.nih.gov/geo/) database. The data from GSE48060 (provided by the GPL570 platform) and GSE60993 (provided by the GPL6884 platform) were obtained from peripheral blood samples of 31 patients with AMI and 21 controls and 17 patients with AMI and 7 controls, respectively. In addition, 2483 immune-related genes and 11,296 inflammation-related genes were retrieved from ImmPort (https://www.immport.org/home) and GeneCards (https://www.genecards.org/) websites, respectively.[12,13]

Identification of Differentially Expressed Immuno-Inflammation-Related Genes (DEIIRGs)
First, we identified differentially expressed genes ($|\text{Log}_2\text{FC}| > 0.5$ and $p < 0.05$) between 31 patients with AMI and 21 controls in GSE48060 data set via "limma" version (v) 3.44.3 and "ggplot2" (v3.3.2) package.[14–16] Further, Venn diagram (http://jvenn.toulouse.inra.fr/) of differentially expressed genes, immune-related genes, and inflammation-related genes was plotted to obtain overlapping genes, which were defined as DEIIRGs.

Enrichment Analysis of DEIIRGs
Gene ontology (GO) function, disease ontology (DO), and Kyoto Encyclopedia of Genes and Genomes (KEGG) pathway enrichment analyses were performed using the DEIIRGs. GO function and KEGG pathway enrichment analyses were performed using the "clusterprofiler" (v3.2–3) package.[17] In our study, KEGG pathway and GO terms with $p < 0.05$ and $q < 0.05$ were retained.[18] A bar plot and dot plot were plotted by the "ggplot2" package for visualization. The genes were annotated from the perspective of diseases using DO. The screening threshold was minGSSize = 5 and $p = 0.05$, and then DO enrichment was analyzed using "DOSE" (v3.24.2) and "clusterProfiler" packages and visualized using the "ggplot2" package.[19]

Screening of Biomarkers and Establishment of Artificial Neural Network (ANN)
Based on the DEIIRGs, a support vector machine recursive feature elimination (SVM-RFE) model and least absolute shrinkage and selection operator (LASSO) model were constructed using the "E1071" (v1.7–9) and "glmnet" (v4.0–2) packages to obtain relevant feature genes.[20,21] To ensure the accuracy of biomarkers, we overlapped the above feature genes identified by the SVM-RFE and LASSO models. The overlapping genes were defined as the biomarkers for AMI. Further, the ANN model was established using the "neuralnet" package (v3.4.2) to further validate the model of biomarkers.[22] The "pROC" (v1.17.0.1) package was used to plot receiver operating characteristic (ROC) curve and calculate area under the curve (AUC) value.[23]

Validation in GSE60993 Dataset

First, Wilcoxon test was performed to compare the expression pattern of biomarkers between AMI and control groups in both GSE48060 and GSE60993 datasets, and the results were mapped as a boxplot using the "ggplot2" package.[24] In addition, principal component analysis (PCA) was used to estimate the ability of biomarkers to differentiate AMI and control groups.[25] Further, the risk scores of biomarkers in both GSE48060 and GSE60993 datasets were calculated as per the method by Hongbo He et al, and the ROC curve was used for determining its reliability.[26]

Construction and Validation of Nomogram

The nomogram of biomarkers was constructed using the "RMS" package (v.6.2–0) (https://CRAN.R-project.org/package=rms). To ulteriorly evaluate its predictive ability for AMI, the calibration curve was plotted with the calibrate function of the "RMS" package. Moreover, the clinical impact curve and decision curve were plotted using the "rmda" package (v1.6) (https://github. com/mdbrown/rmda) to estimate the clinical effect of the nomogram more intuitively.[27]

Ingenuity Pathway Analysis (IPA)

IPA is a multiomics analysis software developed based on the highly structured Ingenuity Knowledge Base repository. Its biggest advantage is the ability to predict pathway activation/inhibition based on the up-down stream molecular in the uploaded data and to predict the trend of the entire pathway after activation. In our study, the canonical pathways of biomarkers were analyzed, where pathways with Z-score > 0 or Z-score < 0 were defined as activated or inhibited, respectively.[28]

Immune Cell Infiltration Analyses

The CIBERSORT method (v1.0.13) was used to assess the immune infiltration of 22 types of immune cells in the AMI and control samples (with $p < 0.05$) from the GSE48060 dataset.[29] Subsequently, Wilcoxon test and the "ggplot2" package were used for the comparative analysis of immune cells between AMI and control groups. The correlation of biomarkers and 22 immune cells was analyzed and visualized using the Pearson method and the "pheatmap" package (v0.7.7).[30,31]

Construction of TF–miRNA–mRNA and Gene–Drug Networks

miRDB (http://www.mirdb.org/mirdb/custom.html) was used to obtain miRNAs targets of the biomarkers. TransmiR v2.0 database (http://www.cuilab.cn/transmir) was used to predict the target TFs of these miRNAs. Furthermore, a TF–miRNA–mRNA network was constructed using Cytoscape (v3.8.2).[32] In addition, the Drug–Gene Interaction Database (DGIdb) (https://dgidb.org/) and Gene Cards (https://www.genecards.org/) database were used to predict the potential therapeutic drugs for the biomarkers. Cytoscape was used to draw and visualize the gene–drug network.

Real-Time Quantitative PCR (RT-qPCR)

The total RNA was extracted from 20 peripheral blood samples (n = 10 for each AMI and control groups) at 4°C using TRIzol kit (Ambion) according to the manufacturer's instructions. Next, the extracted RNA was reverse transcribed into cDNA using the SweScript RT I First strand cDNA Synthesis Kit. GAPDH was used as the housekeeping gene. The primer information is given in Table 1. The reaction mixture for qPCR consisted of 3 μL cDNA, 5 μL 2× Universal Blue SYBR Green qPCR Master Mix, 2 μL primers (10 μM forward and reverse primers 1 μL each). The amplification conditions were 95°C for 1 min, 40 cycles of 95°C for 20s and 55°C for 20s, and 72°C for 30s. The results were analyzed using $2^{-\Delta\Delta Ct}$ method.[33]

Statistical Analysis

Wilcoxon test was used to compare the differences in gene expression and immune cell proportions between AMI and control samples. Statistic analysis on data in RT-qPCR was conducted using t-test. $p < 0.05$ was considered significant.

Table 1 The Primer Sequences of Eight Biomarkers Used in the Real-Time Quantitative PCR (RT-qPCR)

Primer	Sequences
SH2D1B F	CAGGTGAAGGTGAGGGATCG
SH2D1B R	AACCAGGAGGAGAGTAGCCC
ADM F	AGTTGTTCATGCTCTGGCGG
ADM R	CCTGATGTACCTGGGTTCGC
PI3 F	CATCGCTGGGACGCTGGTT
PI3 R	CTGGCTCTTGCGCTTTGAC
MMP9 F	GGTGATTGACGACGCCTTTG
MMP9 R	GGACCACAACTCGTCATCGT
NRG1 F	GAGGTGAGAACGCCCAAGTC
NRG1 R	AAGAAAGCAGCACCAACTGAG
CBLB F	TCACAGGACAGACGAAATCTCA
CBLB R	CTGGAATTGACCATTGGGAAAGA
RORA F	GATGCTTTTGTTCTTACTGGCG
RORA R	CATTGCTTTGCTGACTTCTCCT
FASLG F	TGCCTTGGTAGGATTGGGC
FASLG R	GCTGGTAGACTCTCGGAGTTC
Reference gene-GAPDH F	CGAAGGTGGAGTCAACGGATTT
Reference gene-GAPDH R	ATGGGTGGAATCATATTGGAAC

Abbreviations: AMI, acute myocardial infarction; GEO, gene expression omnibus; DEGs, differentially expressed genes; DEIIRGs, differentially expressed immuno-inflammation-related genes; LASSO, least absolute shrinkage and selection operator; SVM-RFE, support vector machine recursive feature elimination; ANN, artificial neural network; ROC, receiver operating characteristic; AUC, the area under the ROC curve; DCA, decision curve analysis; IPA, ingenuity pathway analysis; CIBERSORT, Cell-type Identification By Estimating Relative Subsets Of RNA Transcripts; TFs, transcription factors; Dgidb, Drug–Gene Interaction Database (DGIdb); qRT-PCR, quantitative real-time polymerase chain reaction.

Ethics Statement
The study complied with the Declaration of Helsinki and was approved by the Ethics Committee of Shaanxi Provincial People's Hospital, Xi'an, Shaanxi, China. Written informed consent was obtained from all study participants.

Results
Identification and Screening of DEIIRGs
In the GSE48060 dataset, 134 differentially expressed genes (40 up- and 94 downregulated) were identified between AMI and control groups (Figures 1A and B). Further, Venn diagram was plotted using 2483 immune-related genes, 134 differentially expressed genes and 11,296 inflammation-related genes to obtain 30 overlapping genes. They were defined as DEIIRGs (Figure 1C).

Enrichment Analysis of DEIIRGs
GO and KEGG enrichment analyses revealed that the DEIIRGs were principally enriched in immune-cell-mediated immunity or cytotoxicity, immune receptor activity, cytokine activity, natural-killer-cell-mediated cytotoxicity pathway,
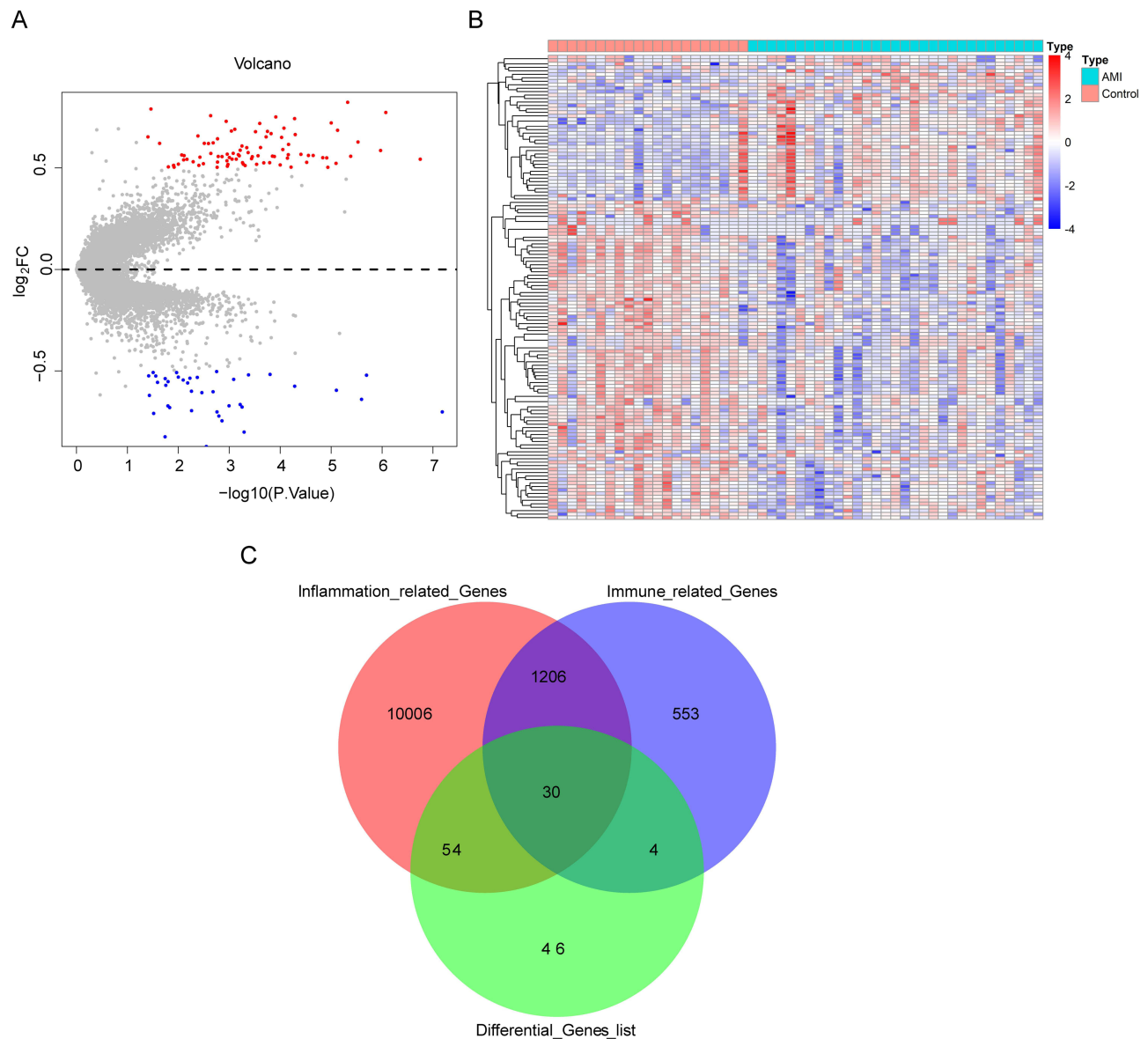
Figure 1 Identification and screening of differentially expressed immuno-inflammation-related genes (DEIIRGs). (**A**) Volcano plot and (**B**) heatmap of 134 differentially expressed genes (DEGs) between acute myocardial infarction (AMI) and control samples in GSE48060. The screening criteria were set to |Log2FC| > 0.5 and $p < 0.05$. (**C**) Venn diagram that obtained 30 DEIIRGs after overlapping 134 DEGs and 11,296 inflammation-related genes.

antigen processing and presentation, cytokine–cytokine receptor interaction, and PI3K-Akt signaling pathway (Figures 2A and B). Notably, DO enrichment analyses indicated that the DEIIRGs were significantly enriched in MI, aortic disease, Kawasaki disease, and blood coagulation disease (Figures 2C and D, Supplementary Table 1).

Identification of Biomarkers and Construction of the ANN Network

Using the LASSO regression model (Figures 3A and B), 10 feature genes (*SH2D1B, ADM, HLA-DQA1, PI3, MMP9, NRG1, XCL1, CBLB, RORA*, and *FASLG*) were identified from the 30 DEIIRGs. In addition, 16 feature genes were screened from the DEIIRGs via the SVM-RFE model (Figures 3C and D). To further verify the biomarkers, Venn diagram was plotted using these feature genes, and eight overlapping genes (*SH2D1B, ADM, PI3, MMP9, NRG1, CBLB, RORA*, and *FASLG*) were selected as the biomarkers for AMI (Figure 3E). They were uploaded into the R software "neuralnet" package, and the ANN model was constructed (Figure 3F). The input of all biomarkers corresponded to an output feature, and the AUC value was 0.709 (Figure 3G). This indicated that the model of biomarkers was reliable.
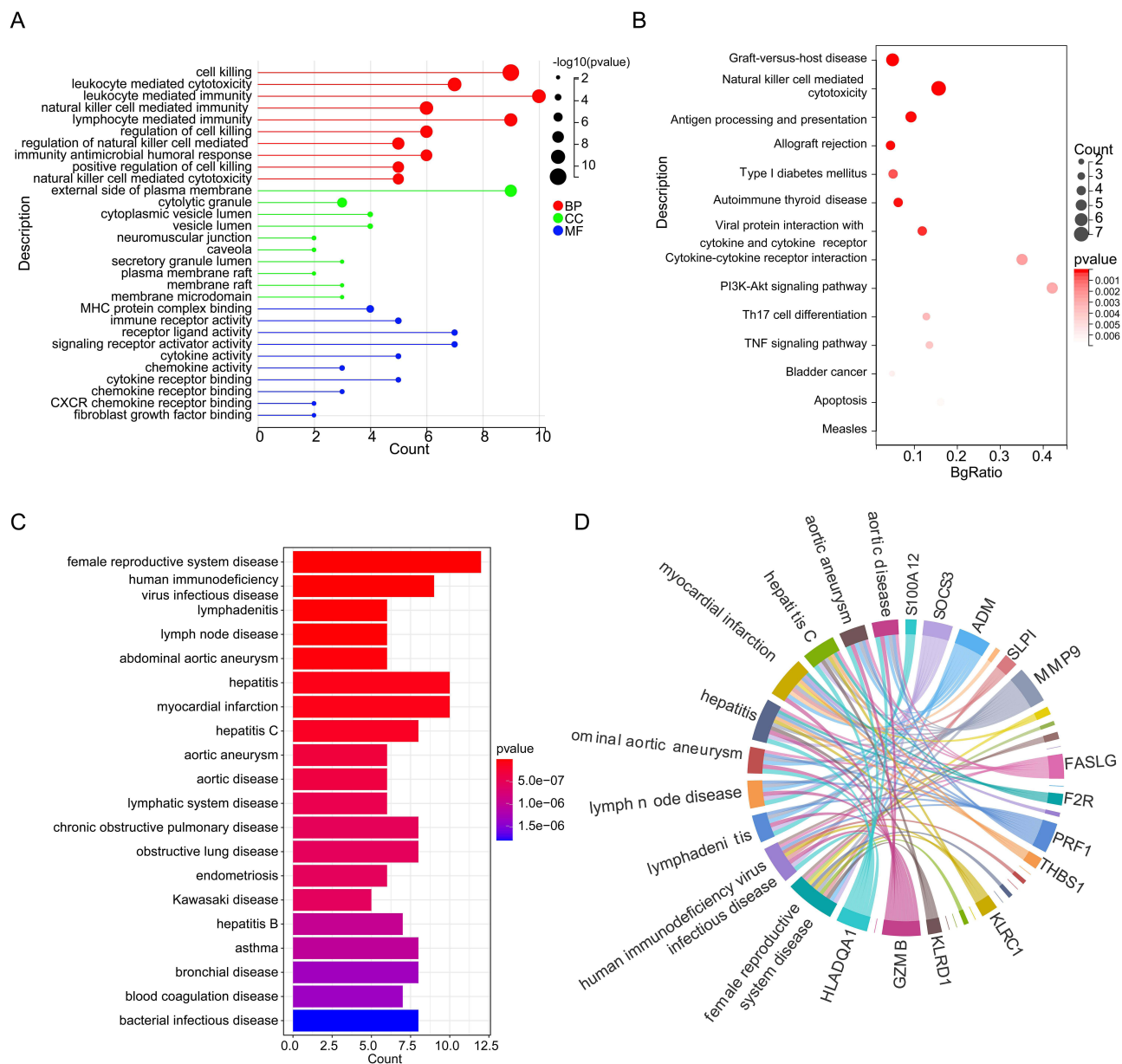
Figure 2 Functional enrichment analysis of DEIIRGs. (**A**) The Gene Ontology (GO) analysis for the DEIIRGs ($p < 0.05$ and $q < 0.05$). (**B**) The most enriched Kyoto Encyclopedia of Genes and Genomes (KEGG) terms for the DEIIRGs. (**C**) Bar chart and (**D**) circle chart for disease ontology (DO) enrichment analysis of the DEIIRGs (minGSSize = 5 and p = 0.05).

Verification of the Eight Biomarkers

In both GSE48060 (Figure 4A) and GSE60993 (Figure 4B) datasets, the expression trend of the biomarkers was consistent. *ADM, MMP9, NRG1* and *PI3* were upregulated in the patients with AMI compared with the control group, whereas other four biomarkers were downregulated. However, the difference in the expression was considerable only in case of *ADM, CBLB, FASLG* and *MMP9*. In addition, PCA revealed that the eight biomarkers performed well in differentiating AMI and control samples in the GSE60993 dataset (Figure 4C). The AUC value of the biomarkers in the GSE48060 and GSE60993 datasets was 0.977 and 0.874, respectively (Figure 4D). In summary, the eight biomarkers exhibited reliability and repeatability in the two datasets.
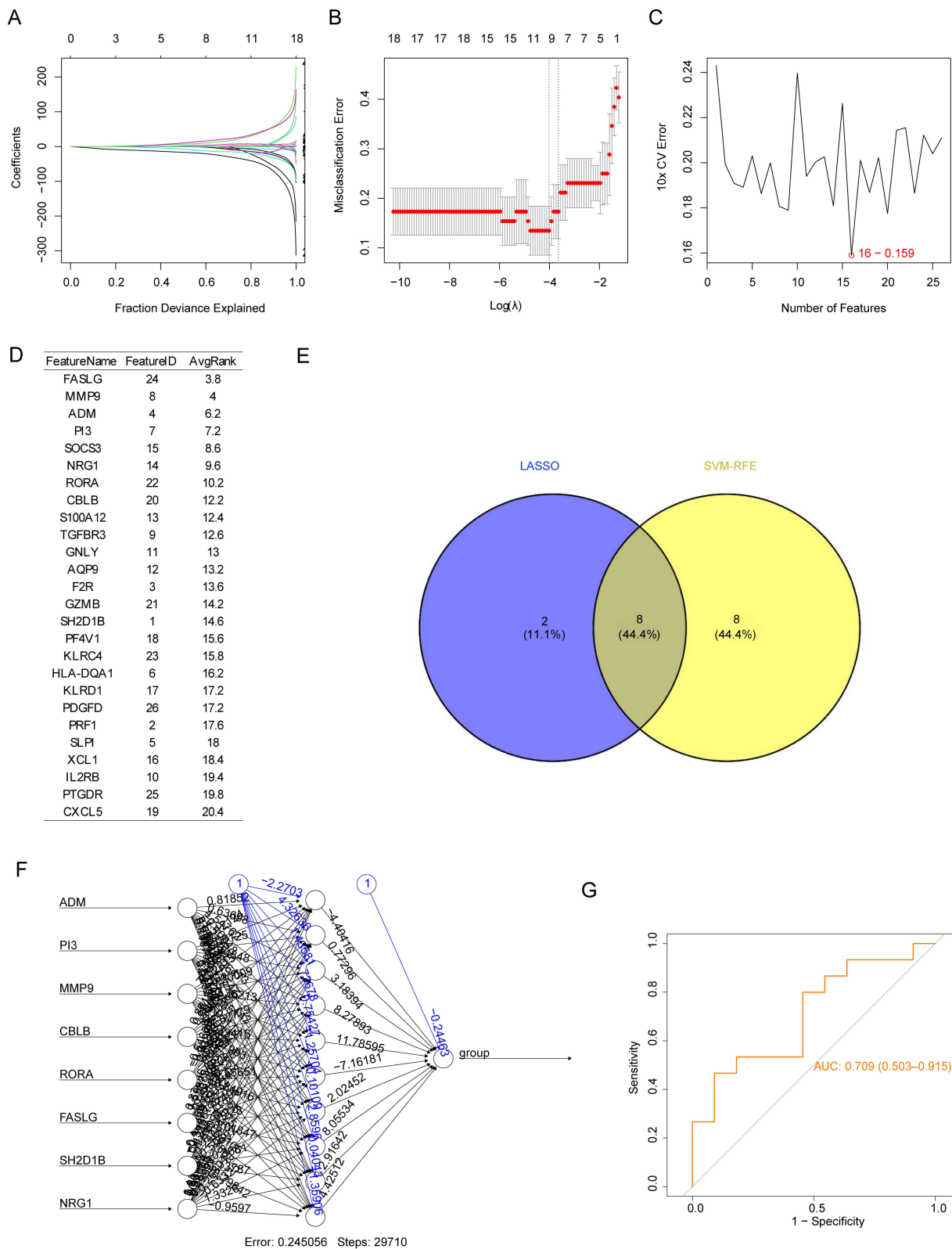
Figure 3 Screening of biomarkers and establishment of artificial neural network (ANN) in GSE48060. (**A**) Ten feature genes were selected by the least absolute shrinkage and selection operator (LASSO) Cox models. (**B**) Cross-validation for tuning parameter selection in the LASSO model. (**C**) 16 feature genes were detected via the support vector machine recursive feature elimination (SVM-RFE) model. (**D**) Feature genes rank in the SVM-RFE model. (**E**) Venn diagrams for eight biomarkers for AMI. (**F**) The ANN model was constructed based on eight biomarkers using "neuralnet". (**G**) Receiver operating characteristic (ROC) curve of the ANN model.
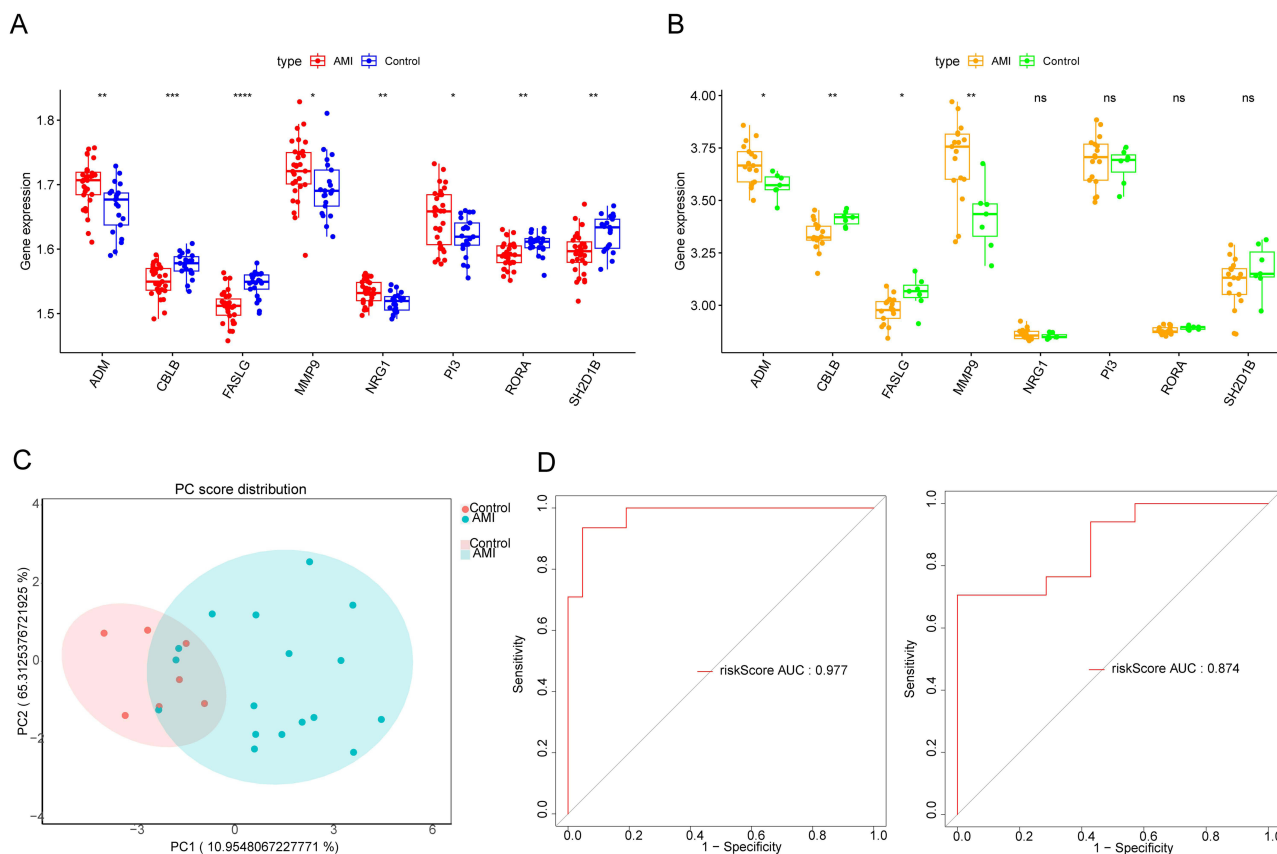
Figure 4 Assessment of the eight biomarkers in GSE48060 and GSE60993 datasets. Boxplot of the expression of eight biomarkers in AMI and control samples in (**A**) GSE48060 and (**B**) GSE60993. (**C**) Principal component analysis (PCA) of GSE60993 based on the expression of biomarkers. (**D**) ROC analysis of the gene signature based on the eight biomarkers using GSE48060 and GSE60993 databases. P < 0.05 was considered in significant difference, where p < 0.05: *, p < 0.01: **, p < 0.001: *** and p < 0.0001: ****.

Construction and Evaluation of the Nomogram

The "RMS" package was used to plot a nomogram of the aforementioned eight genes (Figure 5A). The calibration curve indicated that it accurately predicted AMI (Figure 5B). Within the 0–1 high-risk threshold of the DCA plot, this nomogram benefited, and its benefit was clinically higher than *SH2D1B, ADM, PI3, MMP9, NRG1, CBLB, RORA, and FASLG* (Figure 5C). In addition, from 0 to 1, the curve of "Number high risk" and "Number high-risk with the event" under the high-risk threshold almost coincided (Figure 5D). In summary, all biomarkers exhibited accurate predictability for AMI.

IPA of Biomarkers

IPA analysis was performed to further explore the influence of biomarkers on canonical pathways. *MMP9* was significantly involved in the activation of the neuroprotective role of THOP1 in Alzheimer's disease (Z-score = 2, -log(p-value) = 2.38), FAK signaling (Z-score = 3.051, -log(p-value) = 2.97) (Figure 6A, Supplementary Table 2). *FASLG* was closely associated with the activation of the cytotoxic T lymphocyte-mediated apoptosis of target cells (Z-score = 2, -log(p-value) = 2.71), type I diabetes mellitus signaling (Z-score = 2, -log(p-value) = 3.38), crosstalk between dendritic cells and natural killer cells (Z-score = 2, -log(p-value) = 2.7), and systemic lupus erythematosus in T cell signaling pathways (Z-score = 2.236, -log(p-value) = 2.01). Particularly, FAK Signaling pathway (Z-score = 3.05) was selected to demonstrate the transcriptional role of *MMP9* (Figure 6B).

Evaluation of Immune Cell Infiltration

To compare the immune cell infiltration between AMI and control groups, the proportion of immune cells in 52 samples was calculated (Figure 7A). Wilcoxon test revealed that the infiltration level of monocytes and M0 macrophages was significantly
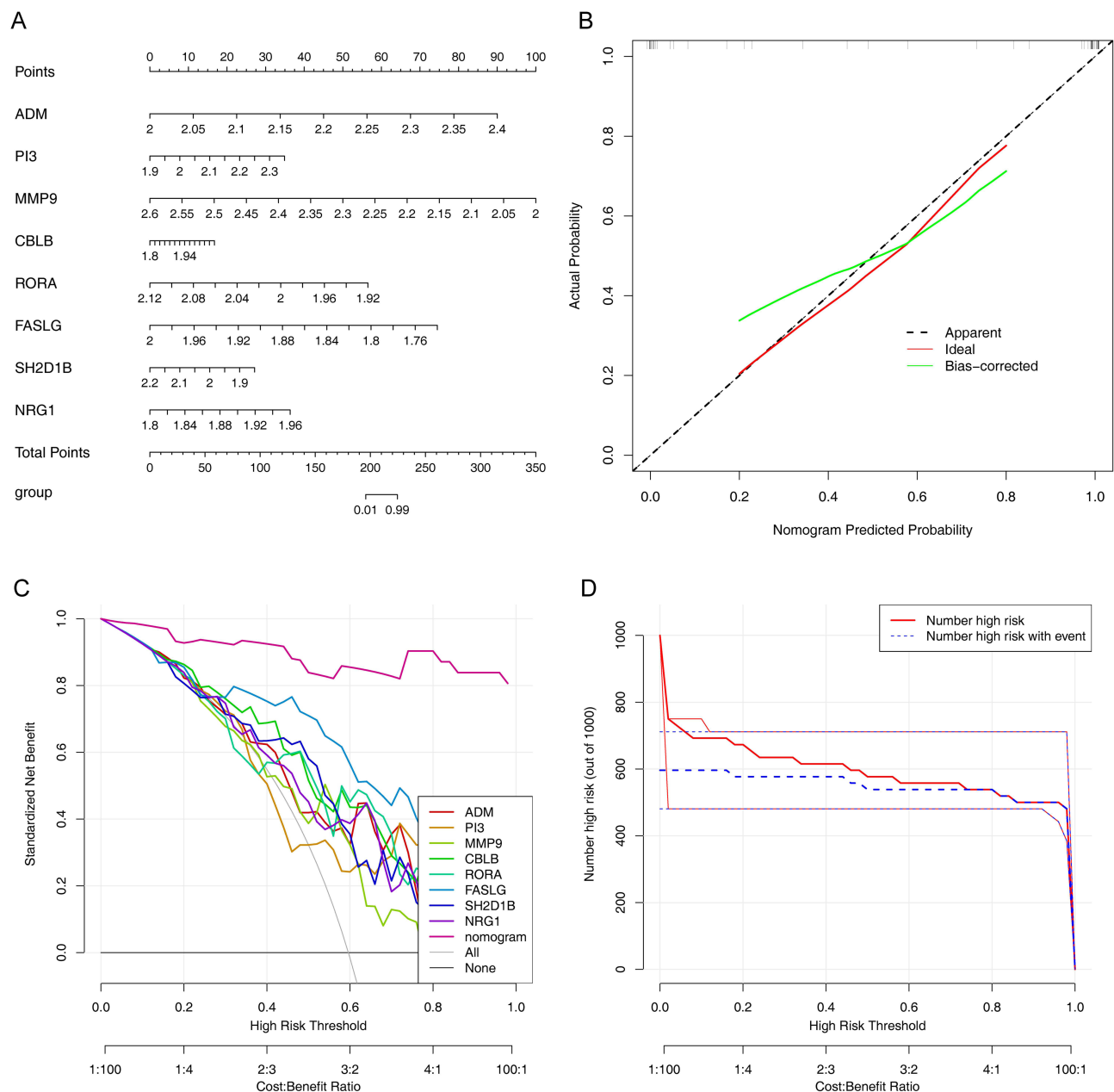
Figure 5 Construction and evaluation of the nomogram. (**A**) Nomogram was constructed based on the eight biomarkers. (**B**) Calibration curve of nomogram (C-index = 0.969278). Clinical benefits of nomogram were evaluated using decision curve analysis (DCA) (**C**) and clinical impact curves (**D**).

higher in AMI group than in control group. However, the infiltration level of Tregs, memory resting CD4+ T-cells and M2 macrophages was significantly lower in AMI group than in control group (Figure 7B). Correlation analysis revealed that M0 macrophages and neutrophils were significantly positively related to *ADM* (cor = 0.631, 0.674) and *MMP9* (cor = 0.781, 0.658). Monocytes were strongly negatively associated with *RORA* (cor = −0.544) and *CBLB* (cor = −0.534) (Figure 7C, Supplementary Table 3).

TF–miRNA–mRNA Regulation Network

In miRDB database, 590 miRNAs potentially targeted by the biomarkers were predicted (33 miRNAs for *ADM*, 114 for *CBLB*, 44 for *FASLG*, 92 for *NRG1*, hsa-mir-6734-3p for *MMP9*, 8 for PI3 and *SH2D1B*, 290 for *RORA*; Supplementary Table 4). Further, the top-5 miRNAs targeting the biomarkers were retained, obtaining 35 miRNAs in total (Supplementary Table 5). After
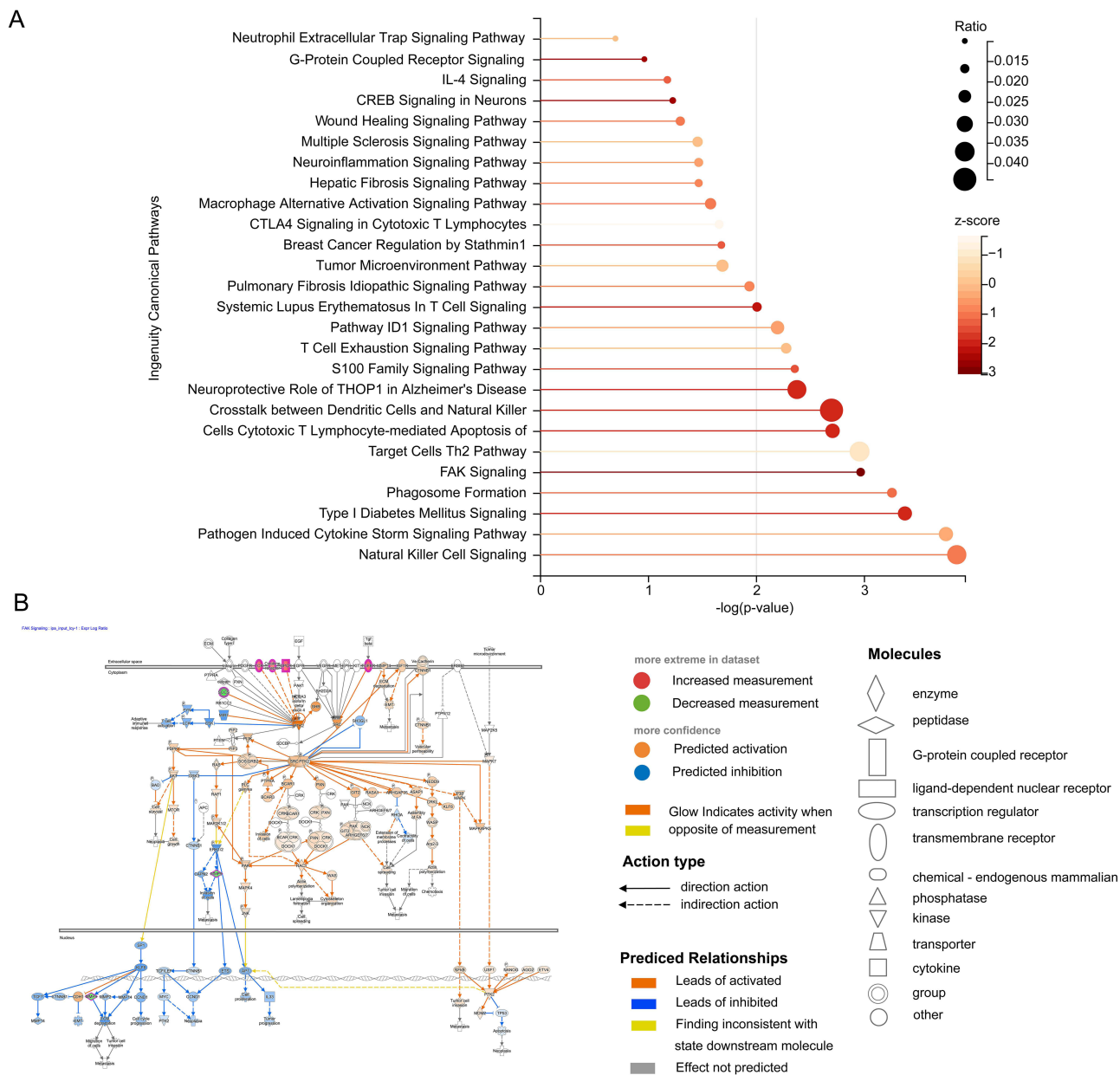
A

B

Figure 6 Ingenuity pathway analysis (IPA) of the biomarkers. (**A**) Bubble chart of enriched canonical pathways. (**B**) The significantly enriched pathway maps of the FAK Signaling pathway.

uploading them on TransmiR v2.0 database, 188 TFs that were the target for hsa-miR-4425, hsa-miR-3920, hsa-miR-1297, hsa-miR-548m, hsa-miR-2052, hsa-miR-548ak, hsa-miR-8485, and hsa-miR-3163 were retrieved. Based on the relationship pairs of TF–miRNA and miRNA–mRNA, a TF–miRNA–mRNA network was constructed (Figure 8).

Potential Therapeutic Drugs of Biomarkers

In Gene Cards database, 140 drugs were predicted that targeted *SH2D1B* [n = 1 (D-tyrosine)], *ADM* (n = 41), PI3 (n = 11), *MMP9* (n = 54), *NRG1* (n = 42), *CBLB* [n = 2 (fluorouracil and D-tyrosine)], *RORA* (n = 9), and *FASLG* (n = 62) (Figure 9A). A total of 27 drugs acting on six biomarkers except *SH2D1B* and *FASLG* were predicted based on the DGIdb database (Figure 9B, Supplementary Table 6). *NRG1* exhibited the strongest interaction with afatinib (interaction score = 1.55). Only one drug
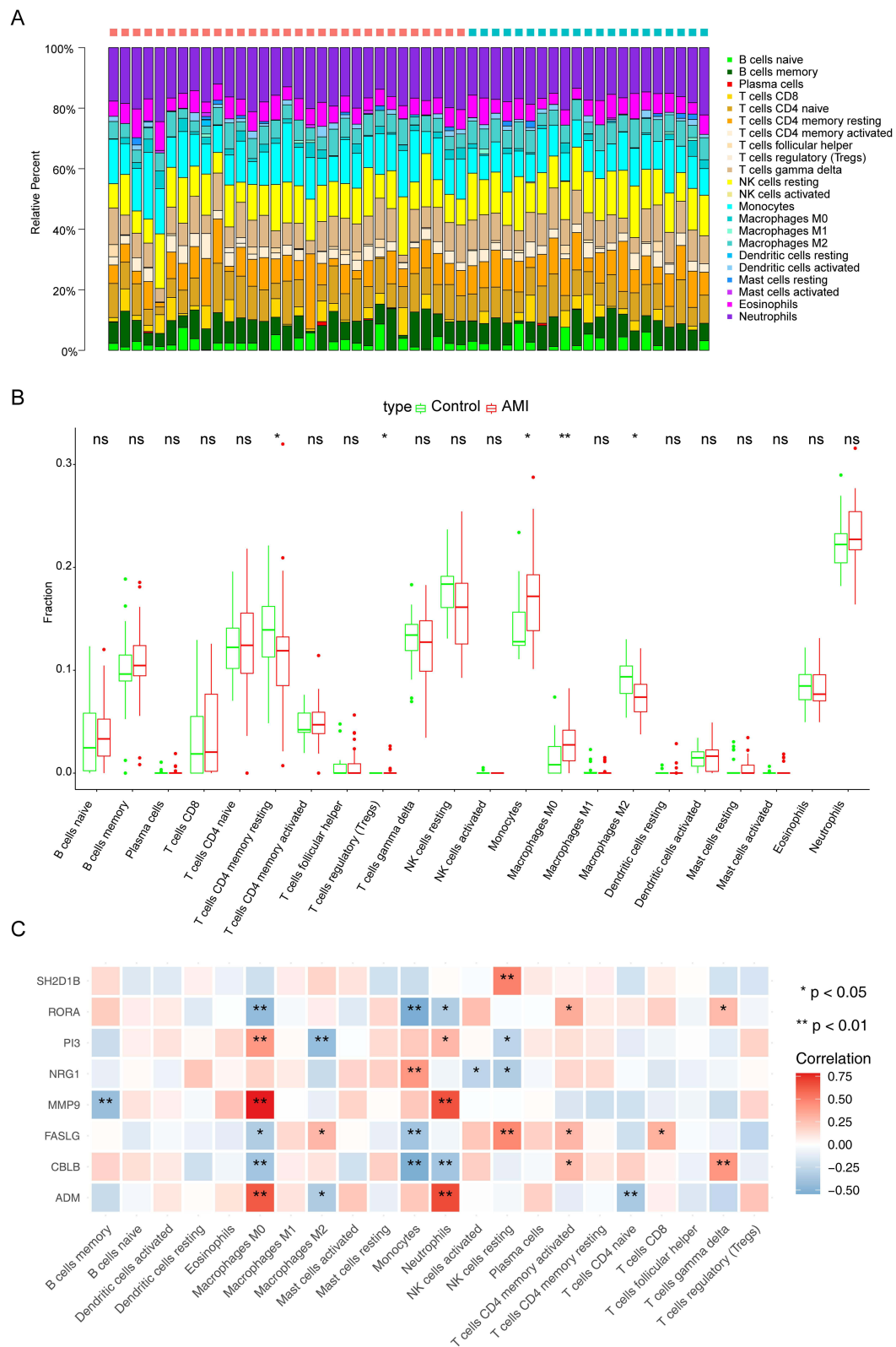
Figure 7 Immune-related analyses targeted biomarkers. (**A**) Histogram for the proportions of 22 immune cells in each patient from GSE48060. Red and cyan represent the AMI and control samples, respectively. The ordinate is the immune cell proportions, and the horizontal axis represents different tissue samples in GSE48060. (**B**) Boxplot of the proportion of immune cells in the AMI and control samples (Wilcoxon test). (**C**) Pearson's correlation heatmap between eight biomarkers and 22 immune cell gene sets. * $p < 0.05$, ** $p < 0.01$.
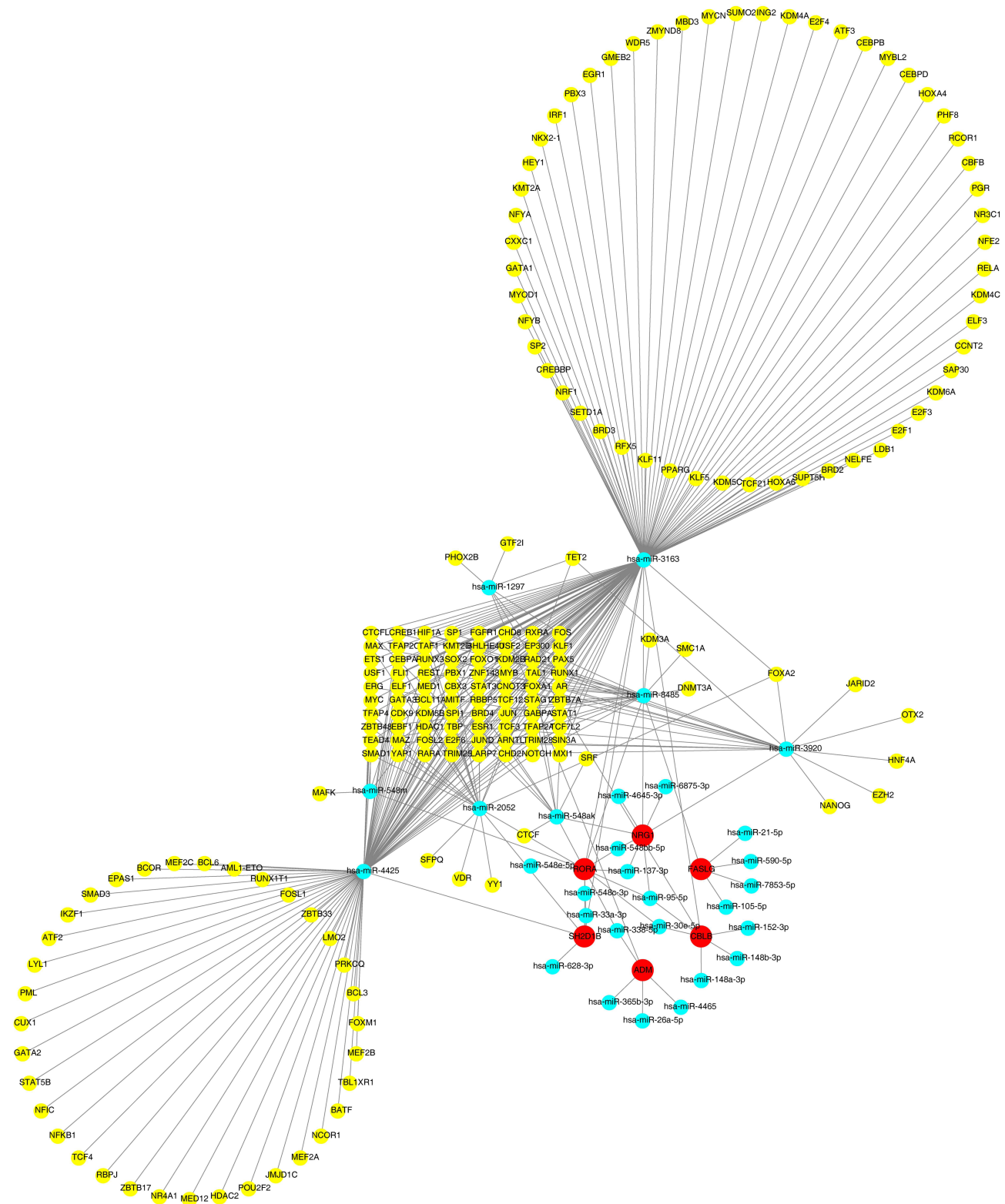
Figure 8 Construction of transcription factor (TF)–miRNA–mRNA networks. Yellow represents TF, blue represents miRNA, and red represent biomarker.

interacted with *PI3* (progesterone; interaction score = 1.85), *CBLB* (fluorouracil; interaction score = 0.59) and *MMP9* (bevacizumab; interaction score = 0.33). For *ADM*, alteplase exhibited the highest interaction score (0.93). Melatonin and citalopram interacted with *RORA* (interaction score = 2.38 and 1.25, respectively).
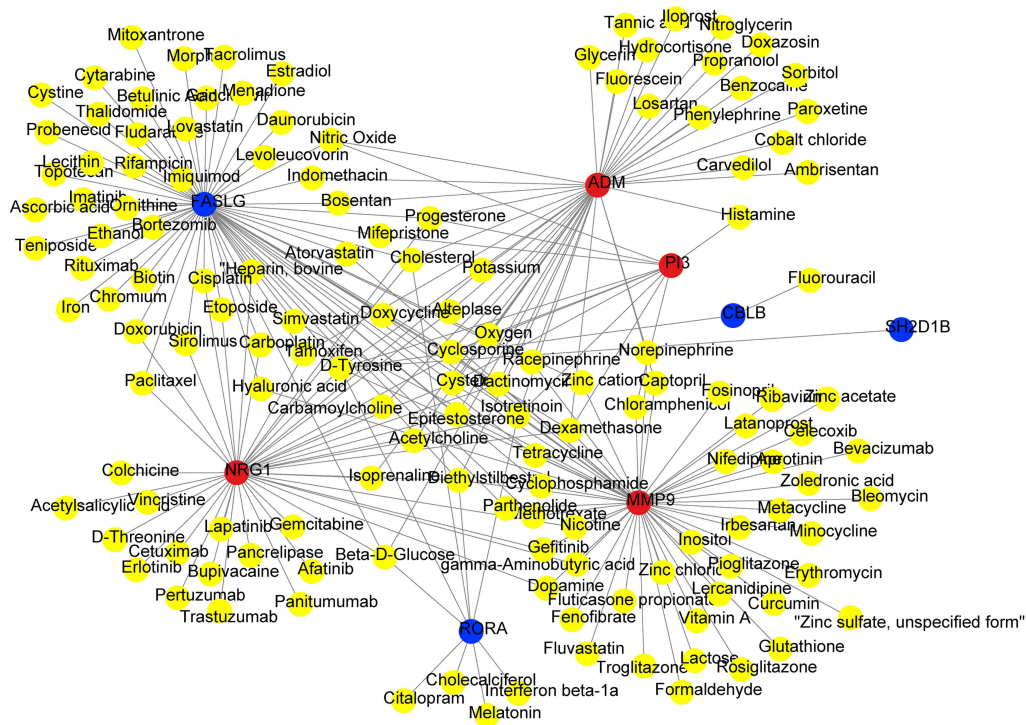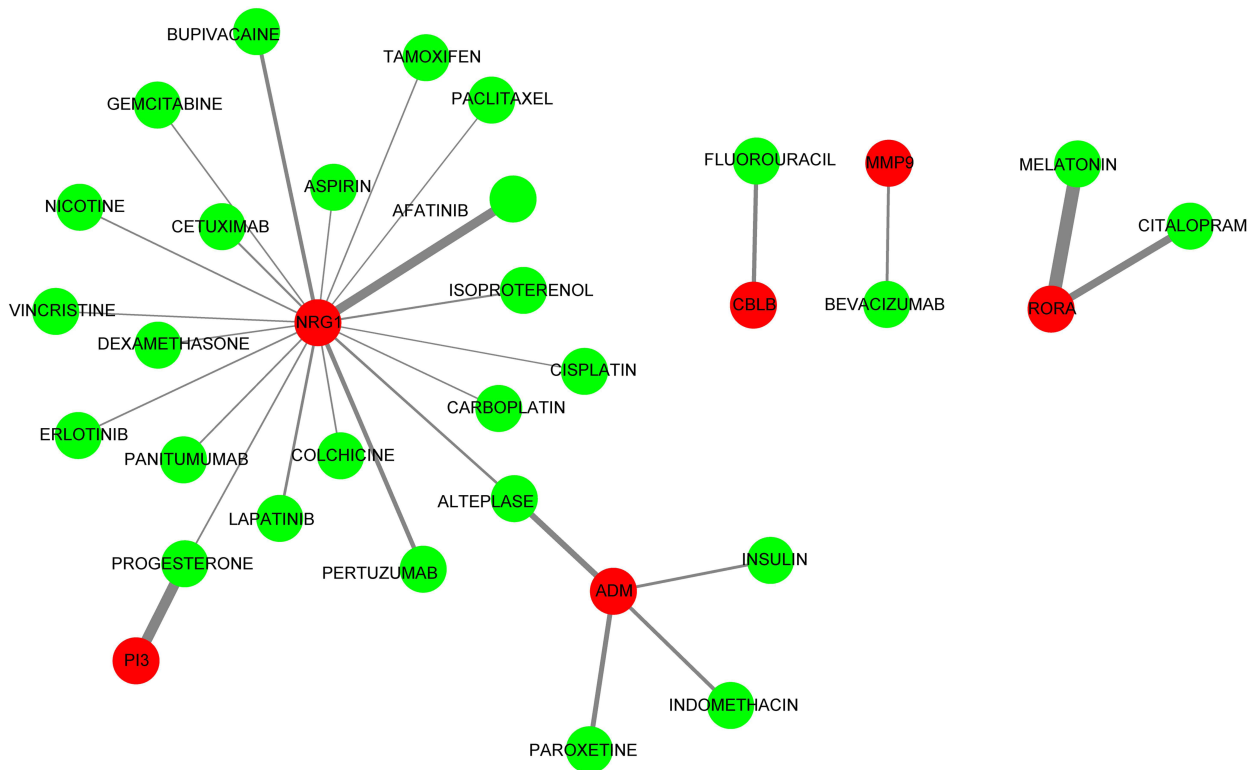
Figure 9 Establishment of the Gene–Drug regulatory networks using Gene Cards database (**A**) and the Drug–Gene Interaction Database (DGIdb) (**B**). Blue represents downregulated biomarker; red represents upregulated biomarker, and yellow and green represent drugs or compounds targeting the biomarkers.
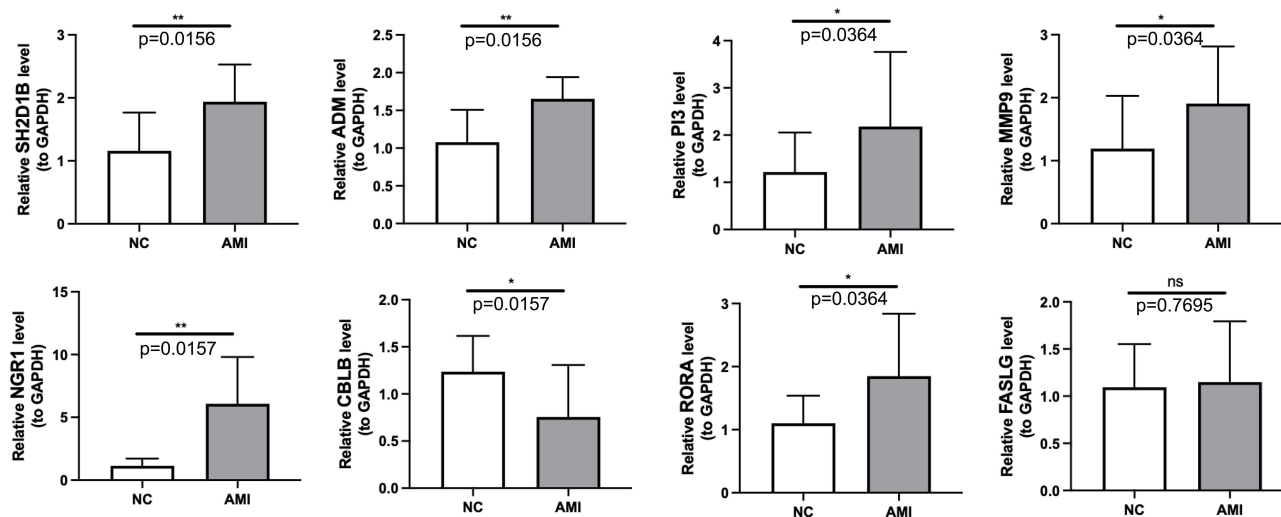
Figure 10 Verification of the eight biomarkers using real-time quantitative PCR (AMI samples = 10, control samples = 10). * *p* < 0.05, ** *p* < 0.01.

RT-qPCR

RT-qPCR revealed that the mRNA level of *SH2D1B, ADM, PI3, MMP9, NRG1*, and *RORA* was higher and that of *CBLC* was lower in AMI group than in control group. The difference in the expression of *FASLG* was not significant in the two groups (Figure 10). However, the results of bioinformatic analysis were contradicting with RT-qPCR results for *SH2D1B* and *RORA*, probably because of the differences in sample size between the data set samples and the experimental samples.

Discussion

Immunity and inflammation are well-established pathways of pathogenesis of AMI. Several biomarkers involving in immune and inflammatory responses are related to the development and progression of AMI.[6,11] In the present study, we used a series of bioinformatic methods to identify immuno-inflammation-related genes involved in AMI and identified the potential biomarkers for AMI. Our study provided new targets for the diagnosis and treatment of AMI and enhanced the understanding of the pathogenesis of AMI.

First, GO, KEGG, and DO enrichment analyses were performed to explore the functions of DEIIRGs. The DEIIRGs were significantly enriched in immune-related biological processes and signaling pathways, such as cell-mediated immunity or cytotoxicity, immune receptor activity, cytokine activity, PI3K/Akt signaling pathway, MI, aortic disease, Kawasaki disease, and blood coagulation disease. Immune cells such as neutrophils and monocytes are prominent participants in inflammation during post-infarction repair.[34,35] Dead cardiomyocytes release danger-associated molecular patterns (DAMPs), which bind to pattern recognition receptors of immune cells. Moreover, myocytes surrounding the infarct core secret DAMPs and proinflammatory cytokines and initiate recruitment of circulating immune cells.[36] Our results revealed that immune cells and responses mediated by their receptors played central roles in AMI. This was consistent with previous studies above. Besides, cytokines are also involved in the pathogenesis of AMI. Proinflammatory cytokines, such as interferon-γ, tumor necrosis factor-α, and interleukins, are the key factors after AMI. Cytokine storm and AMI are mutual cause and effect. Numerous studies have reported the pathogenic effect of cytokine storm in AMI. In addition, cytokine storm after AMI participates in the whole process of AMI from myocardial necrosis to ventricular remodeling.[37] The PI3K/Akt pathway is an important signaling pathway in inflammation.[38] Several studies have reported that the PI3K/Akt signaling pathway could have cardioprotective effects in AMI through many aspects including maintaining endothelial barrier integrity, modulating coagulation and fibrinolysis, and reducing myocardial cell apoptosis.[39–41] Our study verified this. In addition, DO revealed that blood coagulation disease was indicated in the pathogenesis of AMI. Previous studies have established a strong interaction between AMI and blood

coagulation disease.[42] Antithrombotic therapy is important in AMI to avoid thrombotic complications.[43,44] These results provided essential targets for the prevention and treatment of AMI.

Second, the functional analysis of the eight biomarkers was performed. The MMP family is closely related to many cardiovascular diseases. MMP-9 is a well-known enzyme that degrades type-IV collagen of vascular basement membrane and is involved in the whole course of development of atherosclerosis.[45,46] The activation of MMP-9 is associated with poorer prognosis in patients with AMI.[47,48] In addition, therapy with MMP-9 signaling pathway as a target might be a promising option for the treatment of AMI.[49] Our results revealed that the mRNA level of MMP-9 increased in AMI, which is consistent with previous studies. Moreover, our study indicated that MMP-9 was closely related to FAK signaling. FAK, a nonreceptor protein tyrosine kinase, plays diverse roles in cell proliferation, migration and invasion. FAK signaling increases the level of MMP-9.[50] Several studies have reported that FAK signaling is involved in the cell migration of vascular smooth muscle cells, macrophages, and endothelial cell and in decreasing the stiffness of cardiac human fibroblast substrates through MMP-9 upregulation under oxidative stress and hypoxia.[51–54] Based on these, FAK signaling is also recognized as a therapeutic target for atherogenesis and cardiovascular diseases.[55–57] However, evidence of the direct relation among FAK, MMP-9, and AMI is still unavailable, which needs further study. Same as MMP-9, S100 is also one of the biomarkers of AMI as same as MMP-9.[58] Many studies have reported the same trends of change in MMP-9 and S100 in several systemic diseases including diseases of central nervous, digestive, and respiratory systems.[59–61] Meanwhile, *NRG-1* has been reported to play a protective role in AMI by downregulating *MMP-9* expression to alleviate MI-induced cardiac electrical conduction dysfunction.[62] In this study, the simultaneous upregulation of *NRG1* and *MMP-9* genes may imply an imbalance in this regulatory relationship. CBLB, an E3 ubiquitin ligase, is a key inhibitor of transcriptional activity in T cells and a promoter of immune tolerance in innate and adaptive immunity.[63] CBLB$^{-/-}$ murine models demonstrated an inhibitory effect in the case of infections and malignancy.[63] Therefore, targeting CBLB might be an effective strategy to enhance the antitumor activity of T cells.[64,65] To the best of our knowledge, this is the first study to report that the expression of *CBLB* decreases and *ADM*, as well as *HLA-DQA1, PI3* increase in AMI, which has never been reported. The negative regulatory network of hsa-miR-450b-3p-ADM was considered involved in the process of AMI as well, even though that hsa-miR-450b-3p was not predicted by our network.[66] The weak association of *HLA-DQA1* loci with cardiovascular disease has been reported based on 1188 AMI patients and 1191 controls as well.[67] Meanwhile, the relationships of *PI3* and AMI progression remain unclear. It is worth noting that *SH2D1B* was considered to be a potential diagnostic biomarker in HF with depression,[68] which may provide a theoretical basis for the progression of AMI to HF, while the expression patterns of *SH2D1B* in public datasets (downregulation) were different from that in qRT-PCR results (upregulation), as did as RORA. The *RORA* gene was reported to be upregulated in patients with AMI (just like the results of qRT-PCR), which might suppress hypoxic injury of cardiomyocyte cells in AMI by inhibiting oxidative stress and apoptosis.[69,70] Meanwhile, the diagnostic significance of FASLG was detected in AMI,[10] which was consistent with our findings, indicating that these biomarker genes were still worthy of study in AMI.

Third, we tried to investigate the pathogenesis of AMI at the cellular level and observed the differential composition of immune cells between patients with AMI and controls. Previous studies have reported that the percentage of monocytes, particularly proinflammatory monocytes, increases in AMI,[71,72] which is consistent with our study. Particularly, Li et al reported that MMP-9 activity played a pathogenic role in the imbalance of monocytes and macrophages in AMI.[71] It is well established that macrophages participate in the development of atherosclerosis. Macrophages are divided into two polarized subsets: proinflammatory M1 and anti-inflammatory M2 phenotypes.[73] A shift from M2 to M1 phenotype was observed when the atherosclerotic lesions were progressing.[74–76] Proinflammatory macrophages contribute to the plaque destabilization and cause plaque rupture by secreting proinflammatory cytokines and MMP.[77] Our study provided the same results. Hence, promoting the conversion of proinflammatory to anti-inflammatory phenotype is becoming a therapeutic strategy for atherosclerotic diseases.[78–80]

Gene expression is precisely regulated by specific TFs and miRNAs. The dysregulation of upstream TFs and miRNAs of key genes plays a crucial role in the formation and development of cardiovascular diseases. In this study, TF–miRNA–mRNA regulation network was constructed, and some miRNAs were indicated to be related to the aforementioned biomarkers. Luo et al reported that miR-8485 could alleviate the injury of cardiomyocytes in chronic HF.[81] Du reported that miR-3163 could serve as a diagnostic biomarker in coronary artery disease.[82] However, the functions of these miRNAs are almost confined to cancer, and their effects in AMI still need to be explored.

Further, we proposed potential targeted therapeutic drugs for the identified biomarkers. It is well known that premenopausal women show greater resilience against cardiovascular disease than age-matched men, which is widely attributed to estrogen. Many studies have reported that progesterone could attenuate atherosclerosis by inhibiting endothelial cell adhesion and suppressing oxLDL-induced immunity.[83,84] Therefore, some scientists proposed that starting hormone replacement therapy as soon as possible after menopause may prevent atherosclerosis.[85,86] However, some meta-analyses indicated that using oral combined contraceptives is a risk factor for MI and increased susceptibility to cardiovascular disease through upregulating other metabolic disease risk factors.[87] Hence, the use of progesterone to prevent and treat atherosclerosis and AMI still needs to be confirmed. Bevacizumab is a humanized monoclonal antibody that neutralizes the vascular endothelial growth factor (VEGF). It was first approved for the treatment of metastatic colon cancer.[88] Surprisingly, some in vitro and in vivo studies reported that bevacizumab could treat atherosclerosis by inhibiting neovascularization and decreasing total and LDL cholesterol and homocysteine.[89,90] However, some researches reported that systemic VEGF inhibition accelerated atherosclerosis, disrupted endothelial homeostasis, and increased hypertension and arterial thrombotic events.[91,92] Some scientists attempted to use special carriers to transport drug to atheromatous sites precisely.[93,94] This can provide new prospects for the clinical application of bevacizumab in atherosclerosis and AMI. Besides alteplase, a mature thrombolytic agent for treating AMI and acute ischemic stroke,[95,96] two antitumor drugs are also indicated in AMI. 5-fluorouracil is widely used in the treatment of malignancies and has been reported to have side effects on coronary arteries, which is probably attributed to systemic endothelial cell damage and procoagulant state activation.[97] Afatinib has been associated with the development of HF while treating lung cancer.[98] Use of these two drugs in AMI still needs to be further studied.

To further demonstrate the reliability of our results, we collected peripheral blood samples from 10 patients with AMI and 10 healthy controls for RT-qPCR analysis. The results of five of the eight key genes were consistent with the results of bioinformatic analysis. However, the results of *FASLG* and *SH2D1B* were not satisfactorily consistent probably because of the difference in sample size between the two methods, individual differences, and other unknown reasons. This study has some limitations. Our study was performed using public databases and lacked specific clinicopathological information. Further experiments, such as interaction of infiltrating immune cells and key genes, need to be conducted to confirm our findings. Considering a lot of promise of artificial intelligence (AI) systems in coronary syndrome,[99] large quantities of high-quality data and clinical cohorts of AMI were needed to select to verify the predictive efficacy of the diagnostic model.

Conclusion

In conclusion, immuno-inflammation-related genes, *SH2D1B, ADM, PI3, MMP9, NRG1, CBLB, RORA*, and *FASLG*, may serve as the potential biomarkers for AMI, in which the downregulation of *CBLB* and upregulation of *ADM, PI3*, and *NRG1* in AMI were detected for the first time. Meanwhile, the upregulation of *RORA* in RT-qPCR was supported by the literature, providing a new target for the diagnosis and treatment of AMI.

Data Sharing Statement

Publicly available datasets (GSE48060 and GSE60993) were analyzed in this study. These data can be found here: [GEO, https://www.ncbi.nlm.nih.gov/geo/].

Ethics Approval and Informed Consent

The study was conducted in accordance with the Declaration of Helsinki and approved by the Ethics Committee of Shaanxi Provincial People's Hospital. Informed consent was obtained from all subjects involved in the study.

Consent for Publication

Written informed consent has been obtained from the patients to publish this paper.

Author Contributions

All authors made a significant contribution to the work reported, whether that is in the conception, study design, execution, acquisition of data, analysis and interpretation, or in all these areas; took part in drafting, revising or critically reviewing the article; gave final approval of the version to be published; have agreed on the journal to which the article has been submitted; and agree to be accountable for all aspects of the work.

Disclosure

The authors declare that the research was conducted in the absence of any commercial or financial relationships that could be construed as a potential conflicts of interest.

References

1. Anderson HVS, Masri SC, Abdallah MS, et al. 2022 ACC/AHA key data elements and definitions for chest pain and acute myocardial infarction: a report of the American Heart Association/American College of Cardiology Joint Committee on clinical data standards. *J Am Coll Cardiol*. 2022;80(17):1660–1700. doi:10.1016/j.jacc.2022.05.012
2. Tsao CW, Aday AW, Almarzooq ZI, et al. Heart disease and stroke statistics-2023 update: a report from the American Heart Association. *Circulation*. 2023;147(8):e93–e621. doi:10.1161/CIR.0000000000001123
3. Collet JP, Thiele H, Barbato E, et al. 2020 ESC Guidelines for the management of acute coronary syndromes in patients presenting without persistent ST-segment elevation. *Eur Heart J*. 2021;42(14):1289–1367. doi:10.1093/eurheartj/ehaa575
4. Alfonso F, Gonzalo N, Rivero F, Escaned J. The year in cardiovascular medicine 2020: interventional cardiology. *Eur Heart J*. 2021;42 (10):985–1003. doi:10.1093/eurheartj/ehaa1096
5. Guo J, Liu HB, Sun C, et al. MicroRNA-155 promotes myocardial infarction-induced apoptosis by targeting RNA-binding protein QKI. *Oxid Med Cell Longev*. 2019;2019:4579806. doi:10.1155/2019/4579806
6. Torp MK, Vaage J, Stensløkken KO. Mitochondria-derived damage-associated molecular patterns and inflammation in the ischemic-reperfused heart. *Acta Physiol*. 2023;237(3):e13920. doi:10.1111/apha.13920
7. Henein MY, Vancheri S, Longo G, Vancheri F. The role of inflammation in cardiovascular disease. *Int J Mol Sci*. 2022;23(21):12906. doi:10.3390/ijms232112906
8. Andreadou I, Cabrera-Fuentes HA, Devaux Y, et al. Immune cells as targets for cardioprotection: new players and novel therapeutic opportunities. *Cardiovasc Res*. 2019;115(7):1117–1130. doi:10.1093/cvr/cvz050
9. Wang Q, Liu B, Wang Y, Bai B, Yu T, Chu XM. The biomarkers of key miRNAs and target genes associated with acute myocardial infarction. *PeerJ*. 2020;8:e9129. doi:10.7717/peerj.9129
10. Zhang N, Zhou B, Tu S. Identification of an 11 immune-related gene signature as the novel biomarker for acute myocardial infarction diagnosis. *Genes Immun*. 2022;23(7):209–217. doi:10.1038/s41435-022-00183-7
11. Li H, Sun X, Li Z, Zhao R, Li M, Hu T. Machine learning-based integration develops biomarkers initial the crosstalk between inflammation and immune in acute myocardial infarction patients. *Front Cardiovasc Med*. 2023;9:1059543. doi:10.3389/fcvm.2022.1059543
12. Nie H, Yan C, Zhou W, Li TS. Analysis of immune and inflammation characteristics of atherosclerosis from different sample sources. *Oxid Med Cell Longev*. 2022;2022:5491038. doi:10.1155/2022/5491038
13. Xing M, Li J. A new inflammation-related risk model for predicting hepatocellular carcinoma prognosis. *Biomed Res Int*. 2022;2022:5396128. doi:10.1155/2022/5396128
14. Huang Y, Yang DD, Li XY, Fang DL, Zhou WJ. ZBP1 is a significant pyroptosis regulator for systemic lupus erythematosus. *Ann Transl Med*. 2021;9(24):1773. doi:10.21037/atm-21-6193
15. Ritchie ME, Phipson B, Wu D, et al. limma powers differential expression analyses for RNA-sequencing and microarray studies. *Nucleic Acids Res*. 2015;43(7):e47. doi:10.1093/nar/gkv007
16. Ito K, Murphy D. Application of ggplot2 to pharmacometric graphics. *CPT Pharmacometrics Syst Pharmacol*. 2013;2(10):e79. doi:10.1038/psp.2013.56
17. Yu G, Wang LG, Han Y, He QY. clusterProfiler: an R package for comparing biological themes among gene clusters. *Omics*. 2012;16(5):284–287. doi:10.1089/omi.2011.0118
18. Tan R, Zhang G, Liu R, et al. Identification of early diagnostic and prognostic biomarkers via WGCNA in stomach adenocarcinoma. *Front Oncol*. 2021;11:636461. doi:10.3389/fonc.2021.636461
19. Schriml LM, Arze C, Nadendla S, et al. Disease ontology: a backbone for disease semantic integration. *Nucleic Acids Res*. 2012;40:D940–6. doi:10.1093/nar/gkr972
20. Friedman J, Hastie T, Tibshirani R. Regularization paths for generalized linear models via coordinate descent. *J Stat Softw*. 2010;33(1):1–22. doi:10.18637/jss.v033.i01
21. Yang L, Pan X, Zhang Y, et al. Bioinformatics analysis to screen for genes related to myocardial infarction. *Front Genet*. 2022;13:990888. doi:10.3389/fgene.2022.990888
22. Guerriero S, Pascual M, Ajossa S, et al. Artificial intelligence (AI) in the detection of rectosigmoid deep endometriosis. *Eur J Obstet Gynecol Reprod Biol*. 2021;261:29–33. doi:10.1016/j.ejogrb.2021.04.012
23. Robin X, Turck N, Hainard A, et al. pROC: an open-source package for R and S+ to analyze and compare ROC curves. *BMC Bioinform*. 2011;12:77. doi:10.1186/1471-2105-12-77
24. Dexter F. Wilcoxon-Mann-Whitney test used for data that are not normally distributed. *Anesth Analg*. 2013;117(3):537–538. doi:10.1213/ANE.0b013e31829ed28f

25. Abdelhafez OH, Othman EM, Fahim JR, et al. Metabolomics analysis and biological investigation of three Malvaceae plants. *Phytochem Anal*. 2020;31(2):204–214. doi:10.1002/pca.2883

26. He H, Zhang P, Li F, Zeng C, Liu D, Wu K. Predicting the prognosis of esophageal cancer based on extensive analysis of new inflammatory response-related signature. *J Biochem Mol Toxicol*. 2023;37(4):e23291. doi:10.1002/jbt.23291

27. Pan X, Jin X, Wang J, Hu Q, Dai B. Placenta inflammation is closely associated with gestational diabetes mellitus. *Am J Transl Res*. 2021;13 (5):4068–4079.

28. Shao Z, Wang K, Zhang S, et al. Ingenuity pathway analysis of differentially expressed genes involved in signaling pathways and molecular networks in RhoE gene-edited cardiomyocytes. *Int J Mol Med*. 2020;46(3):1225–1238. doi:10.3892/ijmm.2020.4661

29. Chen B, Khodadoust MS, Liu CL, Newman AM, Alizadeh AA. Profiling Tumor Infiltrating Immune Cells with CIBERSORT. *Methods Mol Biol*. 2018;1711:243–259.

30. Pripp AH. Pearsons eller Spearmans korrelasjonskoeffisienter [Pearson's or Spearman's correlation coefficients]. *Tidsskr nor Laegeforen*. 2018;138 (8):1. Danish.

31. Li GM, Zhang CL, Rui RP, Sun B, Guo W. Bioinformatics analysis of common differential genes of coronary artery disease and ischemic cardiomyopathy. *Eur Rev Med Pharmacol Sci*. 2018;22(11):3553–3569. doi:10.26355/eurrev_201806_15182

32. Shannon P, Markiel A, Ozier O, et al. Cytoscape: a software environment for integrated models of biomolecular interaction networks. *Genome Res*. 2003;13(11):2498–2504. doi:10.1101/gr.1239303

33. Livak KJ, Schmittgen TD. Analysis of relative gene expression data using real-time quantitative PCR and the 2(-Delta Delta C(T)) Method. *Methods*. 2001;25(4):402–408. doi:10.1006/meth.2001.1262

34. Zheng PF, Zou QC, Chen LZ, Liu P, Liu ZY, Pan HW. Identifying patterns of immune related cells and genes in the peripheral blood of acute myocardial infarction patients using a small cohort. *J Transl Med*. 2022;20(1):321. doi:10.1186/s12967-022-03517-1

35. Bejjani AT, Saab SA, Muhieddine DH, Habeichi NJ, Booz GW, Zouein FA. Spatiotemporal dynamics of immune cells in early left ventricular remodeling after acute myocardial infarction in mice. *J Cardiovasc Pharmacol*. 2020;75(2):112–122. doi:10.1097/FJC.0000000000000777

36. Weil BR, Neelamegham S. Selectins and immune cells in acute myocardial infarction and post-infarction ventricular remodeling: pathophysiology and novel treatments. *Front Immunol*. 2019;10:300. doi:10.3389/fimmu.2019.00300

37. He W, Chen P, Chen Q, Cai Z, Zhang P. Cytokine storm: behind the scenes of the collateral circulation after acute myocardial infarction. *Inflamm Res*. 2022;71(10–11):1143–1158. doi:10.1007/s00011-022-01611-0

38. Acosta-Martinez M, Cabail MZ. The PI3K/Akt pathway in meta-inflammation. *Int J Mol Sci*. 2022;23(23):15330. doi:10.3390/ijms232315330

39. Liang J, Luo Q, Shen N, et al. PEDF protects endothelial barrier integrity during acute myocardial infarction via 67LR. *Int J Mol Sci*. 2023;24 (3):2787. doi:10.3390/ijms24032787

40. Liberale L, Puspitasari YM, Ministrini S, et al. JCAD promotes arterial thrombosis through PI3K/Akt modulation: a translational study. *Eur Heart J*. 2022;43:1849–1860. doi:10.1093/eurheartj/ehac143

41. Yao E, Luo L, Lin C, et al. OEA alleviates apoptosis in diabetic rats with myocardial ischemia/reperfusion injury by regulating the PI3K/Akt signaling pathway through activation of TRPV1. *Front Pharmacol*. 2022;13:964475. doi:10.3389/fphar.2022.964475

42. Ferreira LGR, Figueiredo RC, Das Graças Carvalho M, Rios DRA. Thrombin generation assay as a biomarker of cardiovascular outcomes and mortality: a narrative review. *Thromb Res*. 2022;220:107–115. doi:10.1016/j.thromres.2022.10.007

43. Sharma C, Osmolovskiy A, Singh R. Microbial fibrinolytic enzymes as anti-thrombotics: production, characterisation and prodigious biopharmaceutical applications. *Pharmaceutics*. 2021;13(11):1880. doi:10.3390/pharmaceutics13111880

44. El Khoury M, Karam B, Tabet R, Lafferty JC, Snyder ST. Current practice of percutaneous coronary intervention in patients with coagulation disorders. *Cureus*. 2021;13(9):e18284. doi:10.7759/cureus.18284

45. Feng B, Li H. Genetic polymorphism of matrix metalloproteinase-9 and susceptibility to myocardial infarction: a meta-analysis. *Dis Markers*. 2022;2022:5507153. doi:10.1155/2022/5507153

46. Nordeng J, Schandiz H, Solheim S, et al. TIMP-1 expression in coronary thrombi associate with myocardial injury in ST-elevation myocardial infarction patients. *Coron Artery Dis*. 2022;33(6):446–455. doi:10.1097/MCA.0000000000001128

47. Domínguez-Rodríguez A, Hernández-Vaquero D, Abreu-González P, et al. Early treatment of acute myocardial infarction with melatonin: effects on MMP-9 and adverse cardiac events. *J Clin Med*. 2022;11(7):248–252. doi:10.3390/jcm11071909

48. Brunton-O'Sullivan MM, Holley AS, Shi B, Harding SA, Larsen PD. Cluster analysis of extracellular matrix biomarkers predicts the development of impaired systolic function within 1 year of acute myocardial infarction. *Heart Vessels*. 2022;37(12):2029–2038. doi:10.1007/s00380-022-02118-8

49. Cheng P, Cheng L, Han H, et al. A pH/H(2) O(2) /MMP9 time-response gel system with sparc(high) tregs derived extracellular vesicles promote recovery after acute myocardial infarction. *Adv Healthc Mater*. 2022;11(22):e2200971. doi:10.1002/adhm.202200971

50. Mon NN, Ito S, Senga T, Hamaguchi M. FAK signaling in neoplastic disorders: a linkage between inflammation and cancer. *Ann NY Acad Sci*. 2006;1086:199–212. doi:10.1196/annals.1377.019

51. Ju S, Lim L, Ki YJ, Choi DH, Song H. Oxidative stress generated by polycyclic aromatic hydrocarbons from ambient particulate matter enhance vascular smooth muscle cell migration through MMP upregulation and actin reorganization. *Part Fibre Toxicol*. 2022;19(1):29. doi:10.1186/s12989-022-00472-z

52. Gałdyszyńska M, Radwańska P, Szymański J, Drobnik J. The stiffness of cardiac fibroblast substrates exerts a regulatory influence on collagen metabolism via α2β1 Integrin, FAK and src kinases. *Cells*. 2021;10(12):3506. doi:10.3390/cells10123506

53. Choi HJ, Kwon I, Kim NE, et al. Fc-saxatilin suppresses hypoxia-induced vascular leakage by regulating endothelial occludin expression. *Thromb Haemost*. 2017;117(3):595–605. doi:10.1160/TH16-06-0469

54. Harada T, Yoshimura K, Yamashita O, et al. Focal adhesion kinase promotes the progression of aortic aneurysm by modulating macrophage behavior. *Arterioscler Thromb Vasc Biol*. 2017;37(1):156–165. doi:10.1161/ATVBAHA.116.308542

55. Nimgulkar C, Ghosh S, Sankar AB, et al. Combination of spices and herbal extract restores macrophage foam cell migration and abrogates the athero-inflammatory signalling cascade of atherogenesis. *Vascul Pharmacol*. 2015;72:53–63. doi:10.1016/j.vph.2015.02.014

56. Coelho NM, Llopis-Hernández V, Salmerón-Sánchez M, Altankov G. Dynamic reorganization and enzymatic remodeling of type IV collagen at cell-biomaterial interface. *Adv Protein Chem Struct Biol*. 2016;105:81–104.

57. Zadeh FJ, Mohammadtaghizadeh M, Bahadori H, Saki N, Rezaeeyan H. The role of exogenous Fibrinogen in cardiac surgery: stop bleeding or induce cardiovascular disease. *Mol Biol Rep*. 2020;47(10):8189–8198. doi:10.1007/s11033-020-05880-y

58. Aydin S, Ugur K, Aydin S, Sahin İ, Yardim M. Biomarkers in acute myocardial infarction: current perspectives. *Vasc Health Risk Manag*. 2019;15:1–10. doi:10.2147/VHRM.S166157

59. Zielińska-Turek J, Dorobek M, Turek G, et al. MMP-9, TIMP-1 and S100B protein as markers of ischemic stroke in patients after carotid artery endarterectomy. *Pol Merkur Lekarski*. 2022;50(297):177–182.

60. Priego-Ranero Á, Opdenakker G, Uribe-Uribe N, et al. Autoantigen characterization in the lower esophageal sphincter muscle of patients with achalasia. *Neurogastroenterol Motil*. 2022;34(9):e14348. doi:10.1111/nmo.14348

61. Railwah C, Lora A, Zahid K, et al. Cigarette smoke induction of S100A9 contributes to chronic obstructive pulmonary disease. *Am J Physiol Lung Cell Mol Physiol*. 2020;319(6):L1021–l35. doi:10.1152/ajplung.00207.2020

62. Yang G, Wu C, Li L, et al. Neuregulin-1 protects cardiac electrical conduction through downregulating matrix metalloproteinase-9 and upregulating connexin 43 in a rat myocardial infarction model. *Pharmazie*. 2019;74(4):231–234. doi:10.1691/ph.2019.8941

63. Augustin RC, Bao R, Luke JJ. Targeting Cbl-b in cancer immunotherapy. *J Immunother Cancer*. 2023;11(2):L1021–L1035. doi:10.1136/jitc-2022-006007

64. Sitaram P, Uyemura B, Malarkannan S, Riese MJ. Beyond the cell surface: targeting intracellular negative regulators to enhance T cell anti-tumor activity. *Int J Mol Sci*. 2019;20(23):5821. doi:10.3390/ijms20235821

65. Fujiwara M, Anstadt EJ, Clark RB. Cbl-b deficiency mediates resistance to programmed death-ligand 1/programmed death-1 regulation. *Front Immunol*. 2017;8:42. doi:10.3389/fimmu.2017.00042

66. Yin X, Wang X, Wang S, et al. Screening for regulatory network of miRNA-inflammation, oxidative stress and prognosis-related mRNA in acute myocardial infarction: an in silico and validation study. *Int J Gen Med*. 2022;15:1715–1731. doi:10.2147/IJGM.S354359

67. Björkbacka H, Lavant EH, Fredrikson GN, et al. Weak associations between human leucocyte antigen genotype and acute myocardial infarction. *J Intern Med*. 2010;268(1):50–58. doi:10.1111/j.1365-2796.2009.02209.x

68. Huang K, Zhang X, Duan J, et al. STAT4 and COL1A2 are potential diagnostic biomarkers and therapeutic targets for heart failure comorbided with depression. *Brain Res Bull*. 2022;184:68–75. doi:10.1016/j.brainresbull.2022.03.014

69. Meng H, Ruan J, Tian X, Li L, Chen W, Meng F. High retinoic acid receptor-related orphan receptor A gene expression in peripheral blood leukocytes may be related to acute myocardial infarction. *J Int Med Res*. 2021;49(6):3000605211019663. doi:10.1177/03000605211019663

70. Cai X, Zhang P, Wang S, et al. lncRNA FGD5 antisense RNA 1 upregulates RORA to suppress hypoxic injury of human cardiomyocyte cells by inhibiting oxidative stress and apoptosis via miR-195. *Mol Med Rep*. 2020;22(6):4579–4588. doi:10.3892/mmr.2020.11558

71. Li JN, Luo RY, Luo C, et al. Brain-derived neurotrophic factor precursor contributes to a proinflammatory program in monocytes/macrophages after acute myocardial infarction. *J Am Heart Assoc*. 2023;12(6):e028198. doi:10.1161/JAHA.122.028198

72. Shen WY, Luo C, Reinaldo Hurtado P, et al. The regulatory role of ProBDNF in monocyte function: implications in Stanford type-A aortic dissection disease. *FASEB J*. 2020;34(2):2541–2553. doi:10.1096/fj.201901905RR

73. Suzuki M, Katayama T, Suzuki C, Nakajima K, Magata Y, Ogawa M. Uptake of nicotinic acetylcholine receptor imaging agent is reduced in the proinflammatory macrophage. *Nucl Med Biol*. 2021;102–103:45–55. doi:10.1016/j.nucmedbio.2021.09.003

74. Bazzi S, Frangie C, Azar E, Daher J. The effect of myeloperoxidase-oxidized LDL on THP-1 macrophage polarization and repolarization. *Innate Immun*. 2022;28(2):91–103. doi:10.1177/17534259221090679

75. Kadl A, Meher AK, Sharma PR, et al. Identification of a novel macrophage phenotype that develops in response to atherogenic phospholipids via Nrf2. *Circ Res*. 2010;107(6):737–746. doi:10.1161/CIRCRESAHA.109.215715

76. Khallou-Laschet J, Varthaman A, Fornasa G, et al. Macrophage plasticity in experimental atherosclerosis. *PLoS One*. 2010;5(1):e8852. doi:10.1371/journal.pone.0008852

77. Libby P, Ridker PM, Hansson GK. Progress and challenges in translating the biology of atherosclerosis. *Nature*. 2011;473(7347):317–325. doi:10.1038/nature10146

78. Profumo E, Maggi E, Arese M, et al. Neuropeptide Y promotes human M2 macrophage polarization and enhances p62/SQSTM1-dependent autophagy and NRF2 activation. *Int J Mol Sci*. 2022;23(21):13009. doi:10.3390/ijms232113009

79. Jing Y, Gao B, Han Z, Xin S. HOXA5 induces M2 macrophage polarization to attenuate carotid atherosclerosis by activating MED1. *IUBMB Life*. 2021;73(9):1142–1152. doi:10.1002/iub.2515

80. Marengo B, Bellora F, Ricciarelli R, et al. Oxysterol mixture and, in particular, 27-hydroxycholesterol drive M2 polarization of human macrophages. *Biofactors*. 2016;42(1):80–92.

81. Luo X, Xu Y, Zhong Z, Xiang P, Wu X, Chong A. miR-8485 alleviates the injury of cardiomyocytes through TP53INP1. *J Biochem Mol Toxicol*. 2022;36(10):e23159. doi:10.1002/jbt.23159

82. Du Y, Yang SH, Li S, et al. Circulating MicroRNAs as novel diagnostic biomarkers for very early-onset (≤40 years) coronary artery disease. *Biomed Environ Sci*. 2016;29(8):545–554. doi:10.3967/bes2016.073

83. Pang Y, Thomas P. mPRα and PR co-operate in progesterone inhibition of endothelial cell focal adhesion. *J Mol Endocrinol*. 2023;70(1):e220073. doi:10.1530/JME-22-0073

84. Groh LA, Verel DE, van der Heijden C, et al. Immune modulatory effects of progesterone on oxLDL-induced trained immunity in monocytes. *J Leukoc Biol*. 2022;112(2):279–288. doi:10.1002/JLB.3AB1220-846R

85. Fait T. Prescription rules of hormone replacement therapy and its alternative. *Cas Lek Cesk*. 2023;161(7–8):309–313.

86. Karim R, Xu W, Kono N, et al. Effect of menopausal hormone therapy on arterial wall echomorphology: results from the Early versus Late Intervention Trial with Estradiol (ELITE). *Maturitas*. 2022;162:15–22. doi:10.1016/j.maturitas.2022.02.007

87. Fuller KNZ, McCoin CS, Stierwalt H, et al. Oral combined contraceptives induce liver mitochondrial reactive oxygen species and whole-body metabolic adaptations in female mice. *J Physiol*. 2022;600(24):5215–5245. doi:10.1113/JP283733

88. De Falco S. Antiangiogenesis therapy: an update after the first decade. *Korean J Intern Med*. 2014;29(1):1–11. doi:10.3904/kjim.2014.29.1.1

89. Li Y, Zhu Y, Deng Y, et al. The therapeutic effect of bevacizumab on plaque neovascularization in a rabbit model of atherosclerosis during contrast-enhanced ultrasonography. *Sci Rep*. 2016;6:30417. doi:10.1038/srep30417

90. Melichar B, Kalábová H, Krcmová L, et al. Serum homocysteine, cholesterol, retinol, alpha-tocopherol, glycosylated hemoglobin and inflammatory response during therapy with bevacizumab, oxaliplatin, 5-fluorouracil and leucovorin. *Anticancer Res*. 2009;29(11):4813–4820.

91. Winnik S, Lohmann C, Siciliani G, et al. Systemic VEGF inhibition accelerates experimental atherosclerosis and disrupts endothelial homeostasis--implications for cardiovascular safety. *Int J Cardiol*. 2013;168(3):2453–2461. doi:10.1016/j.ijcard.2013.03.010

92. Touyz RM, Herrmann SMS, Herrmann J. Vascular toxicities with VEGF inhibitor therapies-focus on hypertension and arterial thrombotic events. *J Am Soc Hypertens*. 2018;12(6):409–425. doi:10.1016/j.jash.2018.03.008

93. De Negri Atanasio G, Ferrari PF, Baião A, et al. Bevacizumab encapsulation into PLGA nanoparticles functionalized with immunouteroglobin-1 as an innovative delivery system for atherosclerosis. *Int J Biol Macromol*. 2022;221:1618–1630. doi:10.1016/j.ijbiomac.2022.08.063

94. Sutton JT, Haworth KJ, Shanmukhappa SK, et al. Delivery of bevacizumab to atheromatous porcine carotid tissue using echogenic liposomes. *Drug Deliv*. 2016;23(9):3594–3605. doi:10.1080/10717544.2016.1212441

95. Tsivgoulis G, Katsanos AH, Sandset EC, et al. Thrombolysis for acute ischaemic stroke: current status and future perspectives. *Lancet Neurol*. 2023;22(5):418–429. doi:10.1016/S1474-4422(22)00519-1

96. Kunamneni A, Durvasula R. Streptokinase-A drug for thrombolytic therapy: a patent review. *Recent Adv Cardiovasc Drug Discov*. 2014;9 (2):106–121. doi:10.2174/1574890110999150202150017

97. Zhou F, Zhu X, Liu Y, et al. Coronary atherosclerosis and chemotherapy: from bench to bedside. *Front Cardiovasc Med*. 2023;10:1118002. doi:10.3389/fcvm.2023.1118002

98. Zaborowska-Szmit M, Krzakowski M, Kowalski DM, Szmit S. Cardiovascular complications of systemic therapy in non-small-cell lung cancer. *J Clin Med*. 2020;9(5):1268. doi:10.3390/jcm9051268

99. Hayıroğlu Mİ, Altay S. The role of artificial intelligence in coronary artery disease and atrial fibrillation. *Balkan Med J*. 2023;40(3):151–152. doi:10.4274/balkanmedj.galenos.2023.06042023